The formation of the thumb requires direct modulation of *Gli3* transcription by Hoxa13

Maria Félix Bastida[a,1], Rocío Pérez-Gómez[a,1], Anna Trofka[b], Jianjian Zhu[b], Alvaro Rada-Iglesias[a,c,d], Rushikesh Sheth[a,2], H. Scott Stadler[e], Susan Mackem[b], and Marian A. Ros[a,f,3]

[a]Instituto de Biomedicina y Biotecnología de Cantabria, Consejo Superior de Investigaciones Científicas–Universidad de Cantabria–Sociedad para al Desarollo de Cantabria, 39011 Santander, Spain; [b]Cancer and Developmental Biology Laboratory, Center for Cancer Research, National Cancer Institute, Frederick, MD 21702; [c]Center for Molecular Medicine Cologne, University of Cologne, 50931 Cologne, Germany; [d]Cluster of Excellence Cellular Stress Responses in Aging-Associated Diseases, University of Cologne, 50931 Cologne, Germany; [e]Center for Skeletal Biology, Shriners Hospitals for Children, Portland, OR 97239; and [f]Departamento de Anatomía y Biología Celular, Facultad de Medicina, Universidad de Cantabria, 39011 Santander, Spain

Edited by Neil H. Shubin, University of Chicago, Chicago, IL, and approved December 11, 2019 (received for review November 10, 2019)

In the tetrapod limb, the digits (fingers or toes) are the elements most subject to morphological diversification in response to functional adaptations. However, despite their functional importance, the mechanisms controlling digit morphology remain poorly understood. Here we have focused on understanding the special morphology of the thumb (digit 1), the acquisition of which was an important adaptation of the human hand. To this end, we have studied the limbs of the *Hoxa13* mouse mutant that specifically fail to form digit 1. We show that, consistent with the role of Hoxa13 in *Hoxd* transcriptional regulation, the expression of *Hoxd13* in *Hoxa13* mutant limbs does not extend into the presumptive digit 1 territory, which is therefore devoid of distal *Hox* transcripts, a circumstance that can explain its agenesis. The loss of *Hoxd13* expression, exclusively in digit 1 territory, correlates with increased Gli3 repressor activity, a *Hoxd* negative regulator, resulting from increased *Gli3* transcription that, in turn, is due to the release from the negative modulation exerted by Hox13 paralogs on *Gli3* regulatory sequences. Our results indicate that Hoxa13 acts hierarchically to initiate the formation of digit 1 by reducing *Gli3* transcription and by enabling expansion of the *5′Hoxd* second expression phase, thereby establishing anterior–posterior asymmetry in the handplate. Our work uncovers a mutual antagonism between Gli3 and Hox13 paralogs that has important implications for *Hox* and *Gli3* gene regulation in the context of development and evolution.

limb development | Hox genes | Gli3 | thumb

Many of the genes that play important roles in limb patterning have been identified, yet little is known about how differential gene expression patterns are implemented to lead to specific morphological traits. A critical event in the adaptive evolution of tetrapod limb function has been the establishment of a polarized digit pattern with a distinctive anterior digit enabling grasping motions, and ultimately leading to the formation of an opposable thumb. This has been explained, in part, by recruitment of Sonic hedgehog (Shh) expression to the limb, but the regulatory network ensuring formation of a distinct anterior digit 1 remains poorly understood.

In vertebrates, Hh signaling is transduced by Gli transcription factors (Gli1, Gli2, and Gli3), of which Gli3 plays a predominant role in the developing limb (1). Shh signaling stabilizes full-length Gli3, which works as a mild activator, and prevents its proteolysis to a truncated potent repressor (Gli3R) of Shh-regulated targets that dominates in the absence of Shh signaling (1–3). Thus, whereas digit formation is severely curtailed in the absence of Shh (4–6), complete loss of Gli3 function, as in the *extratoes* spontaneous mutation in mice, results in a dramatic expansion in number of nonpolarized digits reminiscent of ancestral tetrapod polydactylous limbs (7). This polydactylous phenotype is unaltered in compound *Shh;Gli3*-null mutants (2, 3), underscoring the dominant role Gli3R levels play in digit regulation. A gradient of Shh, arising from the zone of polarizing activity (ZPA) in the posterior limb bud, acts both to reduce anterior digit number and to polarize digits by modulating Gli3R. Because Shh suppresses Gli3 processing, Gli3R levels in the limb bud form an opposing gradient to that of Shh.

Other major regulators of digit patterning include the *Hox* genes, in particular, members of the *HoxA* and *HoxD* clusters (8, 9). During tetrapod limb development, *Hoxa* genes are sequentially activated in the distal limb bud (10), but their expression evolves to generate mutually exclusive expression domains of *Hoxa11* and *Hoxa13*. *Hoxa11* becomes confined to the zeugopod (forearm), while *Hoxa13* is expressed in the autopod (hand). *Hoxd* gene expression progresses differently, in 2 successive phases (11, 12). The first phase occurs in the early limb bud, mainly involves *Hoxd4* to *Hoxd11*, and correlates with the specification of the stylopod (upper arm) and zeugopod morphology. The second phase takes place in the autopod, mainly involves *Hoxd10* to *Hoxd13*, correlates with autopod morphology, and separates from the first phase by a band of tissue devoid of *Hoxd* transcripts that corresponds to the wrist/ankle. These precise patterns of expression of both *Hoxa* and *Hoxd* genes rely on complex transcriptional regulation that involves multiple long-range enhancers located within the flanking genomic regions (13, 14).

Significance

To understand the special morphology of the thumb (digit 1), an important adaptation of the human hand, we studied *Hoxa13*-null mice that specifically lack this digit. We show that *Hoxa13* mutant limbs specifically lose *Hoxd13* expression in the presumptive digit 1 region, correlating with increased *Gli3* transcription and Gli3 repressor activity. We also show that Hox13 paralogs regulate *Gli3* transcription by negatively modulating the activity of *Gli3* enhancers. Our results indicate that mutual antagonism between Gli3 and Hox13 paralogs determines the anterior–posterior asymmetry of the handplate and that Hoxa13 acts hierarchically to initiate formation of a digit 1 territory by attenuating *Gli3* transcription and enabling second-phase expansion of *5′Hoxd* expression.

Author contributions: M.F.B., A.R.-I., R.S., S.M., and M.A.R. designed research; M.F.B., R.P.-G., A.T., J.Z., R.S., H.S.S., S.M., and M.A.R. performed research; H.S.S. and S.M. contributed new reagents/analytic tools; M.F.B., R.P.-G., A.T., J.Z., A.R.-I., R.S., H.S.S., S.M., and M.A.R. analyzed data; and M.A.R. wrote the paper.

The authors declare no competing interest.

This article is a PNAS Direct Submission.

[1]M.F.B. and R.P.-G. contributed equally to this work.

[2]Present address: Department of Biomedicine, University of Basel Medical School, 4058 Basel, Switzerland.

[3]To whom correspondence may be addressed. Email: rosm@unican.es.

This article contains supporting information online at https://www.pnas.org/lookup/suppl/doi:10.1073/pnas.1919470117/-/DCSupplemental.

First published January 2, 2020.

In addition, Hoxa13 has recently emerged as a major transcriptional regulator controlling the mutually exclusive *Hoxa11* expression domain through a repressive mechanism (15), as well as the switch from the first to the second phase of *Hoxd* expression (16–18).

Interestingly, the Shh/Gli3 signaling system and Hoxd transcription factors are in constant interplay during limb development. Initially, Hoxd proteins contribute to activate *Shh* transcription (19, 20); subsequently, Shh function is essential to relieve Gli3R repression of *Hoxd* gene second-phase expression, enabling digit formation (2, 3, 21–23). In addition, endogenous limb bud 5′Hoxd proteins interact physically with Gli3 in vivo, which could serve to sequester Gli3R and provide a mechanistic basis for the observed stoichiometric functional antagonism between *Gli3* and *5′Hoxd* genes at the phenotypic level (24). Additionally, high Hoxd12 levels were able to convert Gli3R from a repressor to a transactivator of Gli-regulated targets in transfections, which may also contribute to the regulation of digit patterning (24).

Genetic studies indicate that both *Hoxa/d* paralogs play overlapping and partially redundant roles in regulating limb morphogenesis; for example, Hoxa11/d11 act in concert in the zeugopod, and Hoxa13/d13 act in the autopod (25, 26). Yet, surprisingly, such functional overlap is absent in the regulation of digit 1, which is uniquely affected by the sole absence of Hoxa13, in contrast to other digits (25, 27, 28).

Because of the importance of digit 1, the thumb in the human hand, we have here investigated the mechanistic basis for this absolute Hoxa13 requirement. We report that, in the absence of *Hoxa13*, the expression of *Hoxd13* does not extend into the anterior limb bud, consequently leaving the presumptive territory of digit 1 devoid of any distal *Hox* expression, a circumstance sufficient to prevent digit condensation (25, 29). We also detect increased Gli3R activity in the anterior mesoderm resulting from the loss of the negative regulation exerted by Hoxa13 and Hoxd13 through direct binding to several enhancers in the *Gli3* locus. Our results support a model in which Hoxa13 acts hierarchically to reduce *Gli3* transcription and enable expansion of *5′Hoxd* second phase, thereby establishing anterior−posterior (AP) asymmetry in the handplate.

Results

A Gene Dosage Effect in *Hoxa13* Mutants. *Hoxa13*$^{-/-}$ mutants die at midgestation, due to placental and vascular defects (25, 28, 30). Although it has been reported that a small percentage of *Hoxa13* homozygous mutants survive to adulthood in the C57BL/6J genetic background (27), the oldest homozygous embryos that we recovered in our colony were at embryonic day 16.5 (E16.5), despite being maintained in this genetic background. At this stage, the typical *Hoxa13*-null limb phenotype, consisting of absent digit 1 and syndactyly, was prominent (*SI Appendix*, Fig. S1*A* and refs. 25, 27, and 28). The phenotype becomes noticeable between E11.5 and E12.5 in association with the failure of digit 1 chondrogenic condensation to form as detected by *Sox9*, the earliest marker of chondroprogenitors (*SI Appendix*, Fig. S1*B*). Interestingly, a gene dosage effect for *Hoxa13* was observed in heterozygous embryos as a poorly defined digit 1 condensation that eventually resulted in a mild but consistent digit 1 hypoplasia in adult heterozygotes (*SI Appendix*, Fig. S1 *B* and *C*).

Altered *Hox* Code Expression in the Anterior Limb Bud Mesoderm of *Hoxa13*$^{-/-}$ Mutants. The hallmark of digit 1 is the expression of *Hoxd13* but not the other *5′Hoxd* genes (31). This unique combination of Hox products is achieved during the second phase of *Hoxd* transcription when the expression of *Hoxd13* spreads into the anterior handplate mesoderm, surpassing the anterior limit of *Hoxd11* and *Hoxd12* domains, a situation referred to as reverse collinearity (31). Due to the pivotal role played by Hoxa13 in the transition from phase 1 to phase 2 of *Hoxd* gene expression (16–18), the first phase of expression of *Hoxd11* is abnormally prolonged in *Hoxa13* mutants, especially in digit 1 territory and, the gap between the 2 phases is distally displaced (Fig. 1*A*). This also occurs with the first phase of expression of the more 3′*Hoxd* genes *Hoxd4*, *Hoxd9*, and *Hoxd10*, and with the *Hoxa11* expression domain, which is normally restricted to the zeugopod, but becomes distally displaced in the absence of *Hoxa13* (*SI Appendix*, Fig. S2) (18).

In addition, in *Hoxa13*-null autopods, *Hoxd13* transcription failed to extend into digit 1 territory but remained similar to that of the unperturbed *Hoxd12* (Fig. 1 *B* and *C*). Thus, digit 1 progenitors in *Hoxa13* mutants express an altered Hox code that corresponds to the zeugopod, rather than the autopod, as it includes *Hoxa11* and the first-phase *Hoxd* expression but lacks the characteristic *Hoxd13* expression (15–18). The fact that the prospective digit 1 cells in *Hoxa13*-null embryos are devoid of both Hoxa13 and Hoxd13 products may account for the loss of digit 1, as all digit chondrogenic condensations fail to form in the absence of both *Hox13* paralogs (25, 29).

No differences in the pattern of expression of other markers of the anterior mesoderm such as *Tbx2*, *Tbx3*, and *Alx4*, which are expressed primarily at a proximal level, were observed in *Hoxa13*-null limb buds (*SI Appendix*, Fig. S3). Thus, the gene expression perturbations in *Hoxa13* mutants are a late event, restricted to the autopod, as expected for a gene that is first activated in the forelimb around E10.5 (32).

Increased Gli3R Activity in *Hoxa13*$^{-/-}$ Anterior Mesoderm. Our results indicate that Hoxa13 is required, directly or indirectly, for the normal anterior spread of *Hoxd13*. However, we previously showed that *Hoxd13* is strongly and uniformly expressed all along the AP extent of the handplate in compound *Hoxa13;Gli3* mutants (ref. 29 and *SI Appendix*, Fig. S4). Indeed, in the absence of *Gli3,* the second phase of expression of all 5′*Hoxd* genes occurs

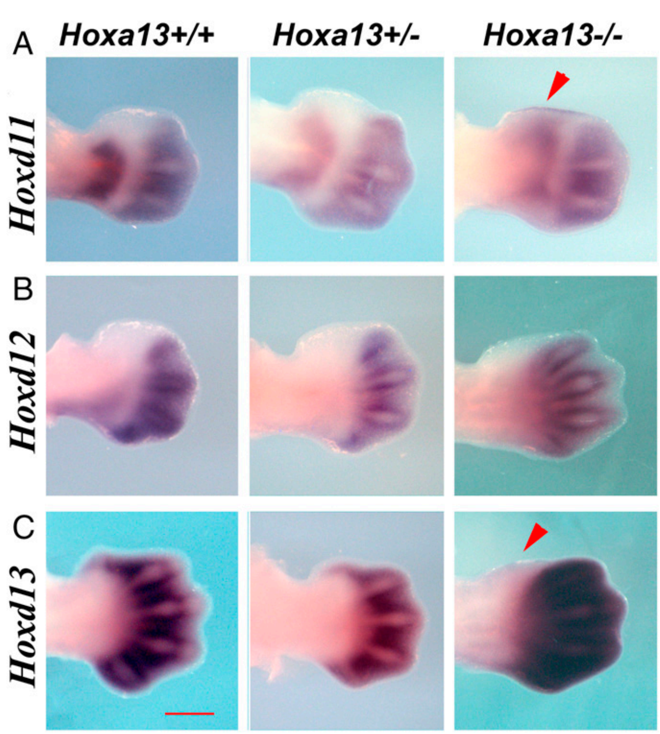

Fig. 1. The *5′Hoxd* gene expression in *Hoxa13* mutant limb buds. Forelimb autopods of wild type and *Hoxa13* heterozygous and *Hoxa13* homozygous mutants hybridized with (*A*) *Hoxd11*, (*B*) *Hoxd12*, and (*C*) *Hoxd13* at E 12.5. The arrowheads point to altered expression patterns in homozygous mutants. (Scale bar: 500 μm.)

DEVELOPMENTAL BIOLOGY

symmetrically all along the AP axis of the handplate, providing a similar Hox code, and presumably a similar amount of Hox products, to all digits (*SI Appendix*, Fig. S4) (2, 3). These considerations suggest that Hoxa13 regulation of *Hoxd13* transcription may be mediated by modulating Gli3 and prompted us to analyze the state of the Gli3R in *Hoxa13* mutants.

RNA in situ hybridization showed up-regulation and distal expansion of the expression domain of *Pax9*, a GLI3R activated target gene (33), while *Jag1*, a GLI3R repressed target gene (33), was absent from the anterior mesoderm of *Hoxa13* mutants at E11.5 and E12.5 (Fig. 2 *A* and *B*). *Bmp4*, a gene whose expression correlates positively with the level of Gli3R (34), showed a more robust and extended domain in the anterior mesoderm (Fig. 2*C*). Overall, these expression pattern modifications are consistent with increased Gli3R activity in the anterior mesoderm of *Hoxa13* mutants. Accordingly, RT-qPCR in dissected E11.75 anterior mesoderm (Fig. 2*D*) showed a 1.7-fold increase in *Gli3* expression ($n = 4$, $P < 0.05$) in *Hoxa13* mutants that was accompanied by a 90% decrease in the level of *Hoxd13* expression ($n = 4$, $P < 0.001$), confirming our in situ hybridization results (Fig. 1*C*). In line with this quantitative increase in transcription, Western blot analysis confirmed a slightly higher level of Gli3R in the anterior limb mesoderm of *Hoxa13* mutant limb buds ($n = 10$, $P < 0.05$; Fig. 2*E*).

Since Gli3 processing depends on Shh activity (35), we investigated the state of the ZPA in *Hoxa13* mutants. In situ hybridization failed to detect any difference in *Shh* expression or signaling (*SI Appendix*, Fig. S5 *A*–*C*). Analysis of the expression of *Fgf8*, the best marker of the apical ectodermal ridge, showed a mild anterior down-regulation in homozygous limb buds that was reflected in reduced *Spry4*, but not *Dusp6* (*SI Appendix*, Fig. S5 *A*, *D*, and *E*). This situation, probably secondary to the increase in *Bmp4*, was also accompanied by a slight down-regulation in the anterior propagation of *Grem1* (*SI Appendix*, Fig. S5*F*). However, these changes did not reach statistical significance when analyzed by RT-qPCR ($P > 0.05$; *SI Appendix*, Fig. S5*G*).

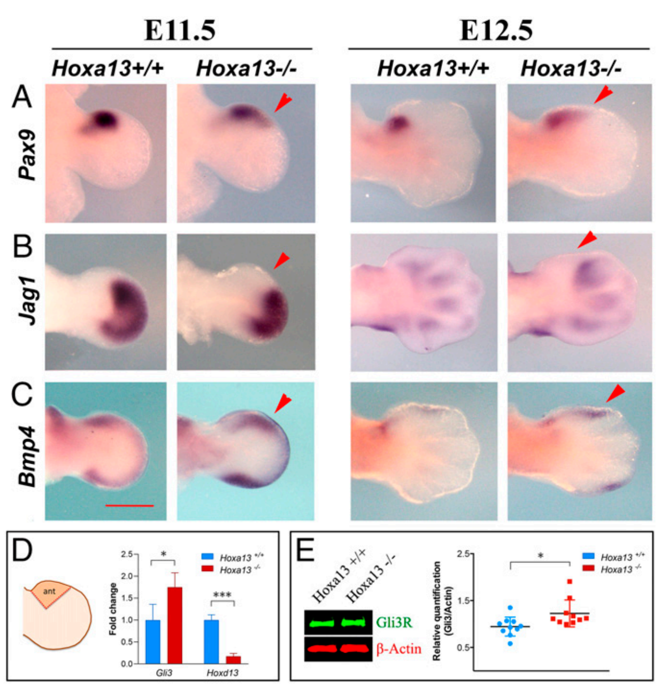

Fig. 2. Expression of Gli3R target genes and quantification of *Gli3* mRNA and protein levels in *Hoxa13* mutant limb buds. Pattern of expression of (*A*) *Pax9*, (*B*) *Jag1*, and (*C*) *Bmp4* in E11.5 and E12.5 forelimb buds of wild type and *Hoxa13* homozygous mutants. Altered expressions are indicated by arrowheads. (Scale bar: 500 μm.) RT-qPCR quantification of (*D*) *Gli3* and *Hoxd13* mRNA and (*E*) Gli3R protein levels in the anterior mesoderm of wild type and *Hoxa13* homozygous mutants. (*$P < 0.05$; ***$P < 0.001$).

Altered *Gli3* Expression Pattern in the Absence of *Hoxa13*. The previous results revealed a moderate excess of *Gli3* transcription and GLI3R protein, and corresponding Gli3R activity in the anterior mutant autopod. To examine in detail how Hoxa13 impacts the overall pattern of *Gli3* expression, we performed a systematic temporal in situ hybridization analysis that exposed a highly dynamic expression pattern. Because of the similarity with 5′*Hoxd* genes, we describe it as evolving in 2 phases (Fig. 3*A*). As reported (23), at E10.5, *Gli3* was expressed in the distal mesoderm, except for the posterior border where *Shh* is expressed. Between E10.5 and E11.5, *Gli3* expression in the distal mesoderm became progressively down-regulated from posterior to anterior until being confined first to the anterior autopod (prospective digit 1 territory) and then to the wrist. By E11.5, a second domain of expression started in the autopod, roughly overlapping digit 4 primordium and progressively propagating anteriorly to cover all of the digit primordia. Therefore, by E12.5, 2 domains of expression, proximal and distal, were clearly distinct and separated by a gap of tissue devoid of transcripts. The proximal domain, a remnant of the first phase of expression, remained as a transverse band at the zeugopod–autopod boundary. The distal domain in the digital plate, corresponding to the second phase of expression, became progressively confined to the interdigital tissue as the digit condensations differentiated (E12.5) and then to the interphalangeal joints (E13.5).

In the absence of *Hoxa13*, the dynamics of *Gli3* expression were dramatically altered from E11, as the down-regulation of the first phase of expression was delayed and incomplete, never reaching the digit 1 territory (Fig. 3*A*). As a consequence, the digit 1 territory remained within the first phase of *Gli3* expression even at later stages, while the second distal domain was restricted to the posterior digits 2 to 4 (schematic summary shown in Fig. 3*B*). This analysis uncovers a previously unidentified hierarchical effect of Hoxa13 in *Gli3* regulation.

The similarity in the expression pattern of *Gli3* and *Hoxd10-11* in E12.5 *Hoxa13* mutants (compare Figs. 3*A* and 1*A*) suggested similar regulation and, considering the cooperation of Hoxd13 with Hoxa13 in regulating *Hoxd* transcription (16–18), pointed to 5′*Hoxd* genes also playing a role in regulating *Gli3* expression. Notably, the analysis of *Gli3* and *Hoxd13* expression in each of the 2 limbs of the same embryo showed that the anterior boundary of *Hoxd13* always abutted the posterior boundary of first-phase *Gli3* expression (Fig. 3*C*), supporting Hoxd13 implication in modulating *Gli3* transcription.

Hox13 Negatively Modulates the Activity of *Gli3* Enhancers. To explore the mechanism for Hoxa13 and Hoxd13 modulation of *Gli3* transcription, we screened the *Gli3* genomic locus for Hoxa13 and Hoxd13 (hereafter conjointly referred to as Hox13) binding sites. We used published datasets of Hox13 DNA binding in limb buds, as well as chromatin state and transcriptome changes between wild type and *Hoxa13;Hoxd13* double mutants (17). We identified several Hox13 binding regions, 4 of which (highlighted in Fig. 4*A*) were also enriched in H3K27ac marks, a mark associated with active enhancers. In agreement with this possibility, 2 of the Hox13 peaks (highlighted in blue in Fig. 4*A*) overlapped with previously reported VISTA enhancers, mm1179 and hs1586, which are active in the limb (36). These observations suggest that Hoxa13 and Hoxd13 could directly regulate *Gli3* transcription, and, based on our in situ and RT-qPCR analyses, this regulation is expected to be negative, consistent with elevated *Gli3* transcript levels (1.7-fold, false discovery rate [FDR] ≤ 0.05) observed in the RNA sequencing (RNA-seq) profiles generated in *Hoxa13;Hoxd13* double-mutant autopods (Fig. 4*A*, 2 bottom tracks) (17).

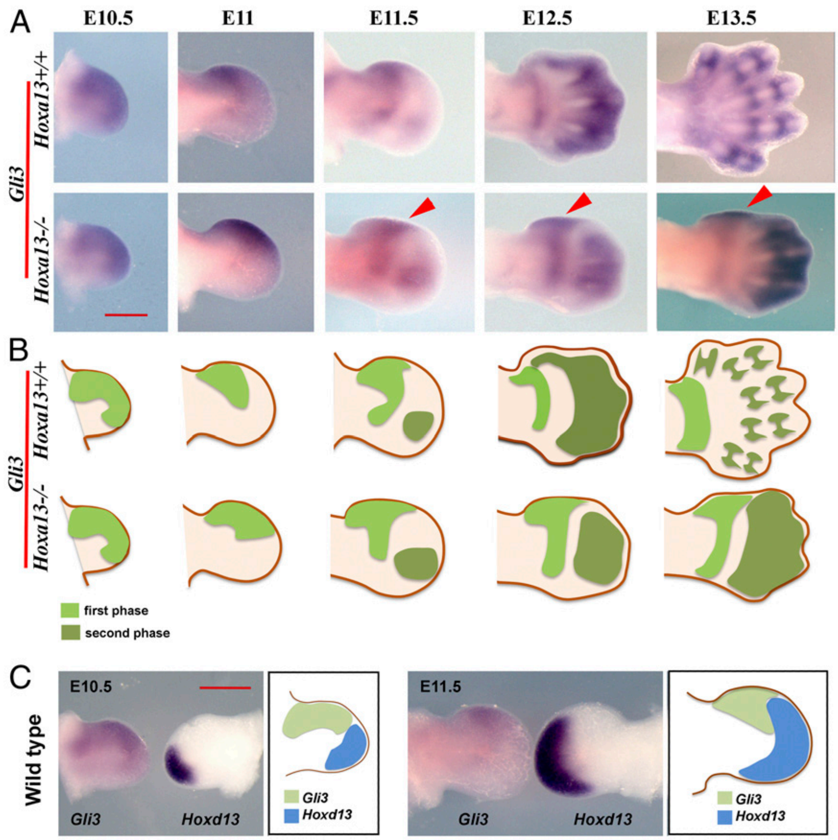

Fig. 3. Dynamics of *Gli3* expression pattern in wild type and *Hoxa13* mutants. (*A*) Expression of *Gli3* during forelimb development in control and *Hoxa13* homozygous mutant limb buds. (*B*) Schematic representation of *Gli3* expression pattern showing phase 1 in lighter green and phase 2 in darker green. (*C*) Comparison of *Gli3* and *Hoxd13* domains of expression in the 2 limb buds of the same wild-type embryo at E10.5 and E11.5 accompanied by an explanatory drawing depicting the abutting of expression domains. (Scale bars: 500 μm.)

To evaluate whether Hox13 proteins can negatively regulate *Gli3* expression through distal enhancer elements, we took advantage of the fact that enhancer activity positively correlates with the generation of short (50 to 2,000 nucleotides) bidirectional transcripts known as enhancer RNAs (eRNAs) (37). Therefore, we measured eRNA levels as a readout of enhancer activity around some of the Hox13 peaks identified within the *Gli3* locus in wild-type and *Hoxa13* mutant contexts. Namely, we analyzed the mm1179 VISTA enhancer and 2 previously undiscovered enhancers, that we called Region I (RI) and Region II (RII), using amplicons located upstream (5′) and downstream (3′) of the corresponding Hox13 peak (primer list in Table 1). Using RT-qPCR, we found that loss of *Hoxa13* significantly increased eRNA levels at the 2 novel putative *Gli3* enhancers analyzed, the 5′ region in RI, and the 3′ region in RII ($n = 3$, $P < 0.05$; Fig. 4*B*). Moreover, a general trend toward increased eRNA levels upon loss of Hoxa13 was also observed for the remaining amplicons. The hs1586 VISTA enhancer was not analyzed, because of its intronic localization that makes its transcription difficult to separate from *Gli3* expression. To further examine the enhancer activity of these novel regions, we used a transient transgenic reporter assay expressing a lacZ cassette under the control of RI or RII. Whole-mount β-galactosidase staining for RII showed reporter activity in the E11.5 limb bud restricted out of the region of *Hox13* expression, as expected for an enhancer whose activity is repressed by Hox13 (2 out of 6; Fig. 4*A*). The RI transgene did not show any activity in the limb, indicating that it may be more context-dependent, for example, requiring other *cis* regulatory elements missing in the transgenic assay, or it might represent a different type of distal regulatory element. Overall, these results indicate that Hoxa13 can negatively modulate the activity of enhancers controlling *Gli3* expression in the autopod, which presumably leads to reduced *Gli3* transcription.

A negative regulation of *Gli3* expression by distal *Hox* genes was also detected in the *Hoxa13*;*Hoxd11-13* allelic series (Fig. 4*C*). In agreement with previous results showing that the absence of *Hoxd11-13* had no major impact on *Gli3* messenger RNA (mRNA) and protein expression (38), our analysis additionally confirmed that the pattern of *Gli3* expression was normal in this mutant (Fig. 4*C*). However, the removal of one functional allele of *Hoxd11-13* from the *Hoxa13*-null background had a stronger impact on *Gli3* expression than the removal of *Hoxa13* alone (Fig. 4*C*). Finally, in the total absence of distal Hox products (*Hoxa13*;*Hoxd11-13* double homozygous mutants), the first phase of *Gli3* expression persisted in the central autopod (Fig. 4*C*). These results support a dose-dependent function of Hoxa13 and 5′Hoxd

Table 1. List of primers used for analysis of eRNA expression

Primer name	Sequence F	Sequence R
RI eRNA5′	GCCCAAGCCCAGTTAATTGT	GAAAATGCACTGGAGGAGGC
RII eRNA5′	AGCAGCTTTTGAAGGCCATC	TGGATCAACTCAGAGCGTGT
RII eRNA3′	ACCCCAACAAGAATCCATGC	TGCAAGTGTTTTCCCCTCTG
mm1179_eRNA5′	TGGGAGGAAGAGTGTTACCG	AGTCCTGTTTTCCTGAGGGG
mm1179_eRNA3′	TGCAAAGTCACAGGCTTCAA	GACATCTTTCACAGCCCAGC

proteins in negatively regulating first-phase *Gli3* transcription. Notably, in preliminary RNA-seq experiments, we observed an increase in *Hoxa13* mRNA, comparing *Hoxd11-13*$^{+/-}$ and *Hoxd11-13*$^{-/-}$ (E12.5 autopod, 1.6-fold, $n = 3$, FDR = 0.008); indeed, comparison of Hoxa13 protein levels (*SI Appendix*, Fig. S6 *A* and *C*) revealed an ∼7-fold increase in *Hoxd11-13* mutants relative to wild-type controls. Given that Hoxa13 and Hoxd13 are known to have redundant functions, this increase in Hoxa13 could compensate for the loss of Hoxd11-13 and explain why the removal of *Hoxd11-13* has no effect on *Gli3* transcription (Fig. 4*C*) or on digit 1 formation.

No Evidence of Hoxa13–Gli3 Physical Interaction. We also considered the possibility that Hoxa13 does not act simply to regulate Gli3 transcription, but by directly interacting with Gli3R protein, as has been shown for 5′ Hoxd11-13 (24). The binding of Hoxa13 protein to GLI3R could modify its activity either by sequestering Gli3R or by transforming its repressor activity into an activator. To test this hypothesis, we performed coimmunoprecipitation (CoIP) of E12.5 limb bud lysates from mice expressing an epitope-tagged allele of Gli3 [3XFLAG-BirA-Gli3 (39, 40)]. No interaction between Hoxa13 and Gli3 was detected, using either immobilized anti-FLAG to coimmunoprecipitate Hoxa13 or using anti-Hoxa13 (17) to coimmunoprecipitate Gli3 (Fig. 4*D*). Additional analysis with a different antibody further confirmed the lack of interaction between Hoxa13 and Gli3 proteins (*SI Appendix*, Fig. S6*B*), supporting the conclusion that the gain in Gli3R activity observed in the anterior autopod of *Hoxa13* mutants results primarily from loss of transcriptional modulation by Hox13 proteins.

Discussion

The thumb, or digit 1, is a crucial adaptation for the functionality of the human hand. It is the last digit to form (41) and the one with higher risk of developmental disruption, with more than 1,000 syndromes in the Online Mendelian Inheritance in Man database, including thumb abnormalities (42). Here, we have used the *Hoxa13*-null mutant that specifically fails to form digit 1, to investigate the mechanisms controlling the formation of this digit.

The Absence of *Hoxd13* Expression in Digit 1 Progenitor Cells Explains Digit 1 Absence in *Hoxa13* Mutants. We show that, in the absence of *Hoxa13*, the *Hoxd13* expression domain in the autopod remains similar to that of *Hoxd12*, without any evidence of the so-called reverse collinearity (31). This is in agreement with the crucial role of Hoxa13 in promoting the second phase of *Hoxd* gene expression (16–18). Thus, in *Hoxa13* mutants, digit 1 territory is devoid of Hox13 paralogs, a situation equivalent to *Hoxa13;Hoxd13* double mutants, that explains the phenotype and highlights the essential function of Hox13 paralogs in the formation of the digital condensations (25, 29). Currently, digit patterning, understood as the generation of a periodic digit–interdigit pattern, is explained by a Turing-type or reaction–diffusion mechanism in which *5′Hox* genes modulate digit spacing, in a dose-dependent manner (29). This model predicts that, in the total absence of distal *Hox* genes (*Hoxa13* and *Hoxd11-13*), the area of digit patterning is strongly reduced, precluding the formation of digital condensations, nicely fitting with the situation selectively observed in digit 1 territory of *Hoxa13* mutants.

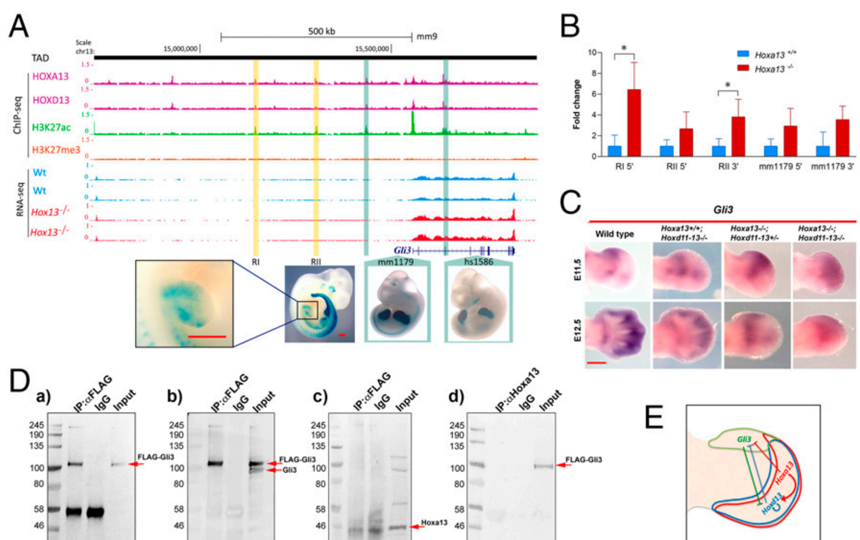

Fig. 4. *Hox13* regulation of *Gli3* expression. (*A*) University of California, Santa Cruz (UCSC) Genome Browser view of the regulatory landscape upstream *Gli3* (16, 17). The black line indicates the extension of the topologically associating domain (TAD) in embryonic stem (ES) cells as in Dixon et al. (45). Chromatin immunoprecipitation (ChIP)-seq tracks for Hoxa13 and Hoxd13 are shown in purple at the top. The H3K27ac and H3K27me3 profiles of the digital plate of E11.5 limb buds are also shown in green and orange, respectively. Two replicates of the transcriptome profiling in wild type (blue) and *Hox13*$^{-/-}$ mutant (red) limb buds at E11.5 are included at the bottom. Two Hox13 binding sites with potential enhancer activity are highlighted in yellow (RI and RII). Two other Hox13 binding sites, highlighted in blue, overlap with 2 previously validated VISTA (36) elements (mm1179 and hs1586), and their activity at E11.5 (Vista Enhancer Browser) is shown below. The activity of RII (LacZ reporter) is also shown, with a magnification of the forelimb. (*B*) Changes in eRNA levels between *Hoxa13*-null and wild-type anterior limb bud mesoderm. The eRNA levels were measured for the indicated enhancers using primers located both upstream (5′) and downstream (3′) of the corresponding Hox13 peaks. The eRNA levels were normalized using *Vimentin* as a housekeeping gene. The eRNA levels 3′ of RI were not measured, since appropriate primers could not be designed. Significance of differences was determined using the 2-tailed, Student's *t* test ($n = 3$; $*P < 0.05$). (*C*) Deregulation of *Gli3* expression in *Hoxa13;Hoxd11-13* compound mutants. Genotype is indicated on the top, and stage is indicated on the left. Note that, while the removal of *Hoxd11-13* has no consequences (second column), its removal in the absence of *Hoxa13* (third column) has a stronger impact in *Gli3* expression pattern than the sole removal of *Hoxa13* (Fig. 3*A*). Finally, in the complete removal of *Hoxa13* and *Hoxd11-13*, *Gli3* expression remains in most of the distal autopod (fourth column). (*D*) FLAG immunoprecipitation of lysates from E12.5 heterozygous 3x-FLAG-Gli3 limb buds immunoblotted with the FLAG antibody showed the Flag-Gli3 band (*a*). Reprobing with an antibody specific for Gli3 additionally showed the wild-type Gli3 band (*b*). The FLAG-Gli3 immunoprecipitates failed to detect CoIP of Hoxa13 using the Hox13 antibody (*c*). Finally, immunoprecipitates using immobilized Hoxa13 antibody and immunoblotted with the FLAG antibody also failed to detect CoIP of the FLAG-Gli3 fusion protein (*d*). (*E*) Schematic diagram indicating the interactions between *Gli3* and *5′Hox* genes. (Scale bars: *A* and *C*, 500 μm.)

***Hoxa13* Mutants Display Elevated Gli3R Activity in the Anterior Mesoderm.** Although Hoxa13 plays a role in the anterior propagation of *Hoxd13*, this function is not required in the absence of *Gli3*. Actually, in the absence of *Gli3*, regardless of whether or not *Hoxa13* is present, the second phase of expression of 5′*Hoxd* genes, including *Hoxd13*, uniformly spans the AP axis of the autopod (refs. 2, 3, 23, and 29 and *SI Appendix*, Fig. S4). Therefore, during normal development, Hoxa13 may function to modulate the repressor function of Gli3R to permit a fully realized second phase of *Hoxd13* expression. Because of its higher transcriptional efficiency, *Hoxd13* is considered to be less sensitive than *Hoxd12* and *Hoxd11* to repression by Gli3R, and therefore is the only 5′*Hoxd* member normally expressed in digit 1, the area of maximum Gli3R activity (31, 35). Thus, Hoxa13 could potentially attenuate Gli3R activity sufficiently to permit the propagation of *Hoxd13*, but not the other 5′*Hoxd* genes, to digit 1 territory, yielding reverse collinearity.

Supporting this hypothesis, we provide compelling evidence of a moderate increase in Gli3R expression and activity in the anterior mesoderm of *Hoxa13* mutants, including elevated *Gli3* transcription and Gli3R protein levels, and altered expression of known Gli3R target genes *Pax9* and *Jag1* (33). Collectively, our results are consistent with an excess of Gli3R in the anterior mesoderm precluding the normal spread of *Hoxd13* expression and subsequent expansion and differentiation of digit 1 progenitors. Because digit 1 is the digit that normally develops with higher Gli3 levels, our results reveal that a balance of Gli3R level is crucial for digit 1 formation. Too much Gli3R precludes anterior spread of *Hoxd13*, leading to the loss of digit 1, while too little also permits *Hoxd12* and *Hoxd11* extension, leading to polydactyly with loss of anteriorization.

Yet digit 1 is the only digit that reportedly forms in the hindlimb with high levels of Gli3R, as occurs in *Shh* and *Ozd* mutants (4–6). However, it should be noted that this hindlimb digit, as well as the small growth that occurs in the *Shh*-null forelimb, is also accompanied by late-stage expression of both *Hoxa13* and *Hoxd13*. Due to the massive cell death that occurs in both *Shh* and *Ozd* mutant limb buds, a cell lineage study would be required to determine the origin of the progenitors of the single rudimentary digit that forms.

Hox13 Paralogs Modulate *Gli3* Transcription. Of note, our analysis also uncovered a previously unappreciated highly dynamic pattern of *Gli3* expression that, due to similarity with 5′*Hoxd* genes, we describe as evolving in 2 phases. The first phase of expression starts in the early limb bud and is then progressively down-regulated from posterior to anterior as the handplate forms, becoming confined to a transverse band at the distal zeugopod. The second phase of expression occurs in the digital plate and is separated from the first phase by a band of tissue devoid of *Gli3* transcripts that corresponds to the wrist/ankle. This dynamic pattern is highly altered in the absence of *Hoxa13,* as the down-regulation of the first phase is delayed and incomplete, resulting in *Gli3* expression remaining over the digit 1 territory. Consequently, when the second phase of expression is established, the gap between the 2 phases lies between prospective digits 1 and 2.

A direct function of Hoxa13 in controlling *Gli3* transcription is supported by the presence of several Hox13 binding sites in the *Gli3* genomic landscape, particularly at 2 novel putative enhancers named RI and RII, identified in this study. Using eRNAs as surrogates of RI and RII activity, we show that Hoxa13 normally reduces RI and RII enhancer activity, providing a mechanism for Gli3R attenuation. Furthermore, the evaluation of RII activity in transient transgenic assays in mice showed limb activity complementary to the area of high *Hox13* expression, in agreement with Hox13 negatively modulating *Gli3* expression and RII activity. In *Hoxa13* mutants, the attenuation of RI and RII enhancer activity is lost, allowing for elevated and prolonged first-phase *Gli3* expression sufficient to disrupt digit I specification.

Notably, in *Hoxa13* mutant autopods, *Gli3* and *Hoxd10* and *Hoxd11* patterns of expression are strikingly comparable. Indeed, the dynamics of the down-regulation of the *Gli3* first phase is totally coincident with the progression of the second phase of *Hoxd13*. This points to a role for *Hoxd13* in attenuating *Gli3* transcription, which is supported by the Hox13 binding sites in the *Gli3* genomic landscape and confirmed by the study of the *Hoxa13;Hoxd11-13* allelic series.

Overall, our study uncovers a level of interaction between *Hox* genes and the Shh/Gli3 pathway: the regulation of *Gli3* transcription by Hox13 paralogs therefore establishing a mutual antagonism that determines the AP asymmetry of the handplate (Fig. 4*E*). Of the 2 Hox13 paralogs, Hoxa13 acts hierarchically to initiate the formation of digit 1 by reducing *Gli3* transcription and by enabling expansion of the 5′*Hoxd* second expression phase (Fig. 4*E*). Consequently, Hoxa13 can compensate for Hoxd13 loss in digit 1 territory, but Hoxd13 cannot compensate Hoxa13 loss, because its expression in that territory is downstream of Hoxa13 activity. On the other hand, Hoxd13 and the 5′Hoxd proteins further modulate Gli3R function through physical interaction (24), an activity that we demonstrate is not shared by Hoxa13.

Materials and Methods

Embryos, Skeletal Preparations, and In Situ Hybridization. The *Hoxa13* (25), $Hoxd^{Del\ (11-13)}$ (43), and $Gli3^{XtJ}$ (7) mutant strains were genotyped by PCR as published. Whole-mount skeletal preparations were performed by staining with Alcian blue 8GX (Sigma Aldrich) and Alizarin red S (Sigma Aldrich) following standard protocols. Whole-mount in situ hybridization was performed according to standard procedures using digoxigenin-labeled antisense riboprobes.

All animal procedures were conducted according to the European Union regulations and 3R principles and reviewed and approved by the Bioethics Committee of the University of Cantabria, and according to the ethical guidelines of the Institutional Animal Care and Use Committee (IACUC) at NCI-Frederick under protocol #ASP-12-405.

Western Blot and qRT-qPCR. For immunoblots, the following antibodies were used: 1) mouse monoclonal Gli3 clone 6F5 anti-Gli3-N antibody, kindly provided by S. Scales at Genentech (44), 2) the goat polyclonal Gli3 (AF3690-SP; R&D Systems), and 3) βactin (C4SC-4778; Santa Cruz) assessed as normalization control. RT-qPCR was carried out on an Applied Biosystems StepOnePlus using SYBR Green Supermix (Bio-Rad), and the data were analyzed with the delta-delta Ct method using the StepOne software (*SI Appendix*). For evaluation of eRNA levels, total RNA was isolated using Tripure reagent according to the manufacturer's instructions (Ref. 11667157001; Roche). Then, total RNA was treated with TURBO DNase-free kit (AM1907; Life Technologies) before complementary DNA synthesis and RT-qPCR. The primers used are listed in Table 1.

CoIP Analysis of Hoxa13 and Gli3. Interaction of Gli3 with Hoxa13 was evaluated by CoIP. A detailed description of the CoIP method is provided in *SI Appendix, Supplementary Materials and Methods*. Briefly, antibodies specific for Hoxa13 (17) and for the FLAG epitope (M2 Sigma F1804) were used to immunoprecipitate Hoxa13 or the FLAG-tagged Gli3 protein from E12.5 limbs heterozygous for a 3XFLAG-Gli3 allele. FLAG-Gli3 immunoprecipitates were evaluated for CoIP of Hoxa13 using the Hoxa13 antibody, and Hoxa13 immunoprecipitates were immunoblotted and assessed for CoIP of the FLAG-Gli3 fusion protein using the FLAG antibody.

Data Availability. All data and materials are available in the main text or *SI Appendix*.

ACKNOWLEDGMENTS. We thank Genentech for the 6F5GLI3 antibody and thank Laura Galán, Mar Rodriguez, and Víctor Campa for excellent technical assistance. We are most grateful to Berta Casar, Lorena Agudo, and Endika Haro for helpful discussions.

1. J. Lopez-Rios, The many lives of SHH in limb development and evolution. *Semin. Cell Dev. Biol.* **49**, 116–124 (2016).
2. Y. Litingtung, R. D. Dahn, Y. Li, J. F. Fallon, C. Chiang, Shh and Gli3 are dispensable for limb skeleton formation but regulate digit number and identity. *Nature* **418**, 979–983 (2002).
3. P. te Welscher *et al*., Progression of vertebrate limb development through SHH-mediated counteraction of GLI3. *Science* **298**, 827–830 (2002).
4. C. Chiang *et al*., Manifestation of the limb prepattern: Limb development in the absence of sonic hedgehog function. *Dev. Biol.* **236**, 421–435 (2001).

5. P. Kraus, D. Fraidenraich, C. A. Loomis, Some distal limb structures develop in mice lacking Sonic hedgehog signaling. *Mech. Dev.* **100**, 45–58 (2001).
6. M. A. Ros *et al*., The chick oligozeugodactyly (ozd) mutant lacks sonic hedgehog function in the limb. *Development* **130**, 527–537 (2003).
7. C. C. Hui, A. L. Joyner, A mouse model of greig cephalopolysyndactyly syndrome: The extra-toesJ mutation contains an intragenic deletion of the Gli3 gene. *Nat. Genet.* **3**, 241–246 (1993).
8. R. Pérez-Gómez, E. Haro, M. Fernández-Guerrero, M. F. Bastida, M. A. Ros, Role of Hox genes in regulating digit patterning. *Int. J. Dev. Biol.* **62**, 797–805 (2018).
9. J. M. Woltering, D. Noordermeer, M. Leleu, D. Duboule, Conservation and divergence of regulatory strategies at Hox Loci and the origin of tetrapod digits. *PLoS Biol.* **12**, e1001773 (2014).
10. Y. Kherdjemil, M. Kmita, Insights on the role of hox genes in the emergence of the pentadactyl ground state. *Genesis* **56**, e23046 (2018).
11. B. Tarchini, D. Duboule, Control of Hoxd genes' collinearity during early limb development. *Dev. Cell* **10**, 93–103 (2006).
12. M. Kmita, N. Fraudeau, Y. Hérault, D. Duboule, Serial deletions and duplications suggest a mechanism for the collinearity of Hoxd genes in limbs. *Nature* **420**, 145–150 (2002).
13. G. Andrey *et al*., A switch between topological domains underlies HoxD genes collinearity in mouse limbs. *Science* **340**, 1234167 (2013).
14. S. Berlivet *et al*., Clustering of tissue-specific sub-TADs accompanies the regulation of HoxA genes in developing limbs. *PLoS Genet.* **9**, e1004018 (2013).
15. Y. Kherdjemil *et al*., Evolution of Hoxa11 regulation in vertebrates is linked to the pentadactyl state. *Nature* **539**, 89–92 (2016).
16. L. Beccari *et al*., A role for HOX13 proteins in the regulatory switch between TADs at the HoxD locus. *Genes Dev.* **30**, 1172–1186 (2016).
17. R. Sheth *et al*., Distal limb patterning requires modulation of cis-regulatory activities by HOX13. *Cell Rep.* **17**, 2913–2926 (2016).
18. R. Sheth, M. F. Bastida, M. Kmita, M. Ros, "Self-regulation," a new facet of Hox genes' function. *Dev. Dyn.* **243**, 182–191 (2014).
19. T. D. Capellini *et al*., Pbx1/Pbx2 requirement for distal limb patterning is mediated by the hierarchical control of Hox gene spatial distribution and Shh expression. *Development* **133**, 2263–2273 (2006).
20. M. Kmita *et al*., Early developmental arrest of mammalian limbs lacking HoxA/HoxD gene function. *Nature* **435**, 1113–1116 (2005).
21. J. P. Lewandowski *et al*., Spatiotemporal regulation of GLI target genes in the mammalian limb bud. *Dev. Biol.* **406**, 92–103 (2015).
22. S. A. Vokes, H. Ji, W. H. Wong, A. P. McMahon, A genome-scale analysis of the cis-regulatory circuitry underlying sonic hedgehog-mediated patterning of the mammalian limb. *Genes Dev.* **22**, 2651–2663 (2008).
23. A. Zúñiga, R. Zeller, Gli3 (Xt) and formin (ld) participate in the positioning of the polarising region and control of posterior limb-bud identity. *Development* **126**, 13–21 (1999).
24. Y. Chen *et al*., Direct interaction with Hoxd proteins reverses Gli3-repressor function to promote digit formation downstream of Shh. *Development* **131**, 2339–2347 (2004).
25. C. Fromental-Ramain *et al*., Hoxa-13 and Hoxd-13 play a crucial role in the patterning of the limb autopod. *Development* **122**, 2997–3011 (1996).
26. A. P. Davis, D. P. Witte, H. M. Hsieh-Li, S. S. Potter, M. R. Capecchi, Absence of radius and ulna in mice lacking hoxa-11 and hoxd-11. *Nature* **375**, 791–795 (1995).
27. W. D. Perez, C. R. Weller, S. Shou, H. S. Stadler, Survival of Hoxa13 homozygous mutants reveals a novel role in digit patterning and appendicular skeletal development. *Dev. Dyn.* **239**, 446–457 (2010).
28. H. S. Stadler, K. M. Higgins, M. R. Capecchi, Loss of Eph-receptor expression correlates with loss of cell adhesion and chondrogenic capacity in Hoxa13 mutant limbs. *Development* **128**, 4177–4188 (2001).
29. R. Sheth *et al*., Hox genes regulate digit patterning by controlling the wavelength of a Turing-type mechanism. *Science* **338**, 1476–1480 (2012).
30. M. Scotti, M. Kmita, Recruitment of 5′ Hoxa genes in the allantois is essential for proper extra-embryonic function in placental mammals. *Development* **139**, 731–739 (2012).
31. T. Montavon, J. F. Le Garrec, M. Kerszberg, D. Duboule, Modeling Hox gene regulation in digits: Reverse collinearity and the molecular origin of thumbness. *Genes Dev.* **22**, 346–359 (2008).
32. W. M. Knosp, C. Saneyoshi, S. Shou, H. P. Bächinger, H. S. Stadler, Elucidation, quantitative refinement, and *in vivo* utilization of the HOXA13 DNA binding site. *J. Biol. Chem.* **282**, 6843–6853 (2007).
33. E. McGlinn *et al*., Pax9 and Jagged1 act downstream of Gli3 in vertebrate limb development. *Mech. Dev.* **122**, 1218–1233 (2005).
34. M. F. Bastida *et al*., Levels of Gli3 repressor correlate with Bmp4 expression and apoptosis during limb development. *Dev. Dyn.* **231**, 148–160 (2004).
35. B. Wang, J. F. Fallon, P. A. Beachy, Hedgehog-regulated processing of Gli3 produces an anterior/posterior repressor gradient in the developing vertebrate limb. *Cell* **100**, 423–434 (2000).
36. A. Visel, S. Minovitsky, I. Dubchak, L. A. Pennacchio, VISTA Enhancer BrowserA database of tissue-specific human enhancers. *Nucleic Acids Res.* **35**, D88–D92 (2007).
37. R. Andersson *et al*., An atlas of active enhancers across human cell types and tissues. *Nature* **507**, 455–461 (2014).
38. B. L. Huang *et al*., An interdigit signalling centre instructs coordinate phalanx-joint formation governed by 5'Hoxd-Gli3 antagonism. *Nat. Commun.* **7**, 12903 (2016).
39. J. Lopez-Rios *et al*., Attenuated sensing of SHH by Ptch1 underlies evolution of bovine limbs. *Nature* **511**, 46–51 (2014).
40. D. S. Lorberbaum *et al*., An ancient yet flexible cis-regulatory architecture allows localized Hedgehog tuning by patched/Ptch1. *eLife* **5**, e13550 (2016).
41. N. B. Fröbisch, R. L. Carroll, R. R. Schoch, Limb ossification in the Paleozoic branchiosaurid *Apateon* (Temnospondyli) and the early evolution of preaxial dominance in tetrapod limb development. *Evol. Dev.* **9**, 69–75 (2007).
42. K. C. Oberg, Review of the molecular development of the thumb: Digit primera. *Clin. Orthop. Relat. Res.* **472**, 1101–1105 (2014).
43. J. Zákány, D. Duboule, Synpolydactyly in mice with a targeted deficiency in the HoxD complex. *Nature* **384**, 69–71 (1996).
44. X. Wen *et al*., Kinetics of hedgehog-dependent full-length Gli3 accumulation in primary cilia and subsequent degradation. *Mol. Cell. Biol.* **30**, 1910–1922 (2010).
45. J. R. Dixon *et al*., Topological domains in mammalian genomes identified by analysis of chromatin interactions. *Nature* **485**, 376–380 (2012).